

Comparative cytotoxicity of *Acanthamoeba castellanii*-derived conditioned medium on human corneal epithelial and stromal cells

Abdullah Alhazmi^{a,b}, Laura E. Sidney^a, Andy Hopkinson^a, Hany M. Elsheikha^{c,*}

^a Academic Ophthalmology, Division of Clinical Neuroscience, University of Nottingham, Nottingham NG7 2UH, UK

^b Faculty of Public Health and Health Informatics, Umm Al Qura University, Makkah, Saudi Arabia

^c Faculty of Medicine and Health Sciences, School of Veterinary Medicine and Science, University of Nottingham, Sutton Bonington Campus, Loughborough LE12 5RD, UK

ARTICLE INFO

Keywords:

Acanthamoeba castellanii
Corneal stromal cells
Corneal epithelial cells
Cytotoxicity
Metabolic activity
Actin cytoskeleton

ABSTRACT

Soluble factors in the secretome of *Acanthamoeba castellanii* play crucial roles in the pathogenesis of *Acanthamoeba* keratitis (AK). Investigating the pathological effects of *A. castellanii*-derived conditioned medium (ACCM) on ocular cells can provide insights into the damage inflicted during AK. This study examined ACCM-induced cytotoxicity in primary human corneal stromal cells (CSCs) and a human SV40 immortalized corneal epithelial cell line (ihCECs) at varying ACCM concentrations (25 %, 50 %, 75 %, and 100 %). MTT, AlamarBlue, Sulforhodamine B, lactate dehydrogenase, and Caspase-3/7 activation assays were used to assess the impact of ACCM on the cell viability, proliferation and apoptosis. Additionally, fluorescent staining was used to reveal actin cytoskeleton changes. ACCM exposure significantly decreased cell viability, increased apoptosis, and disrupted the actin cytoskeleton, particularly at higher concentrations and longer exposures. Proteases were found to mediate these cytopathogenic effects, highlighting the need for characterization of *A. castellanii* proteases as key virulence factors in AK pathogenesis.

1. Introduction

Acanthamoeba keratitis (AK) is a severe corneal infection primarily caused by *Acanthamoeba castellanii*. Other *Acanthamoeba* spp., including *A. culbertsoni*, *A. hatchetti*, *A. griffini*, *A. mauritaniensis*, *A. lugdunensis*, *A. polyphaga* and *A. rhyodes*, have also been implicated in eye infections (Elsheikha et al., 2020). The pathogenesis of AK is partially mediated by soluble factors present in *A. castellanii* secretome (Marciano-Cabral and Cabral, 2003; Carnt et al., 2018). *A. castellanii* is an invasive and persistent parasite, and expresses various virulence proteins, such as the mannose-binding protein, which facilitates adhesion to mannose-glycoproteins on the corneal surface (Garate et al., 2006). Clinical symptoms associated with ocular infection result from inflammation and cellular damage. Misdiagnosis as fungal or viral infection is possible, and any delay in initiating appropriate treatment can have sight-threatening consequences (Jiang et al., 2015). Even with the most potent medications, treatment failure can still occur.

Previous studies have identified various intracellular and extracellular proteases in *Acanthamoeba* species, including cysteine proteases

involved in encystation (Joo et al., 2022; Leitsch et al., 2010; Moon et al., 2012) and host protein hydrolysis (Wang et al. 2020), as well as metalloproteases linked to the pathogenesis of AK and granulomatous amoebic encephalitis (Cao et al., 1998; Kalra et al., 2020; Mahdavi Poor et al., 2023; Sissons et al., 2006). These proteinases exhibit cytopathic effects (CPEs), damaging corneal epithelial cells and the basement membrane, revealing the stromal matrix, and facilitating penetration into the cornea's deeper layers (Cao et al., 1998; Köhler et al., 2016; Mitra et al., 1995).

Most proteolytic enzymes in protozoal extracts demonstrate marked activity across a wide temperature range (8 to 45 °C) and pH levels (3 to 9) (Heredero-Bermejo et al., 2015). An earlier study revealed that heat-resistant molecules with low molecular mass (<10 kDa), released by viable trophozoites of *A. castellanii*, induced several CPEs in an epithelial cell line, such as increase in cytosolic calcium, morphological alterations, cytoskeletal disruption, reduced cell viability, and increased apoptosis, a form of programmed cell death (Mattana et al., 1997). Additionally, *A. castellanii* trophozoites can develop contact-dependent cytolysis, destroying phagocytic cells through cytolytic factors and

* Correspondence author at: Faculty of Medicine and Health Sciences, School of Veterinary Medicine and Science, University of Nottingham, Sutton Bonington Campus, Loughborough LE12 5RD, UK.

E-mail address: Hany.Elsheikha@nottingham.ac.uk (H.M. Elsheikha).

<https://doi.org/10.1016/j.actatropica.2024.107288>

Received 7 April 2024; Received in revised form 10 June 2024; Accepted 11 June 2024

Available online 18 June 2024

0001-706X/© 2024 The Author(s). Published by Elsevier B.V. This is an open access article under the CC BY license (<http://creativecommons.org/licenses/by/4.0/>).

finger-like projections (Marciano-Cabral and Toney, 1998). *A. griffini*, an isolate from a contact lens-wearing patient in Spain, induced focal lesions in HeLa cell monolayers, which were attributed to the activity of serine proteases and cysteine proteases secreted by the amoeba (Here-dero-Bermejo et al., 2015).

Investigation of the factors underlying *A. castellanii*'s CPEs on corneal cells may lead to a better understanding of the mechanisms driving ocular tissue damage. In the present study, we examined the effects of cell-free supernatants from *A. castellanii* culture, termed *A. castellanii*-conditioned medium (ACCM), on the viability, cell death, actin cytoskeleton and ultrastructure of human corneal stromal cells (CSCs) and human SV40 immortalized corneal epithelial cells (ihCECs). Our findings revealed that ACCM significantly reduces cell viability, increases cell death rates, disrupts the actin cytoskeleton and induces morphological alterations at the subcellular level. Moreover, we show that the CPEs induced by ACCM are primarily mediated by proteases. The results provide new insight into the extent of cellular damage caused by the secretome of *A. castellanii*, highlighting the intricate mechanisms underlying its pathogenicity.

2. Materials and methods

2.1. Cell lines and culture conditions

2.1.1. Culture of ihCECs

The human SV40 immortalized corneal epithelial cell line (ihCEC) was established in 1995 by Araki-Sasaki from primary human corneal epithelial cells (Araki-Sasaki et al., 1995). This cell line was kindly provided by Prof. Felicity Rose (University of Nottingham, UK) to the Academic Ophthalmology Department. The ihCECs were transformed using the early region of the Simian virus (SV) 40 genome. The cells were cultured in EpiLife™ medium (Life Technologies, UK), supplemented with penicillin (20 Units/mL), streptomycin (20 µg/mL) and amphotericin B (50 ng/mL) (AbAm, Sigma Aldrich, UK), and 1 % (v/v) human keratinocyte growth supplement (HKGS, Life Technologies, UK). Cultures were maintained at 37 °C in a humidified atmosphere with 5 % CO₂. The medium was changed every 2–3 days. At 90 % confluence, cells were passaged using TryPLE express (Life Technologies, UK).

2.1.2. Isolation and culture of CSCs

Anonymized corneoscleral rims left after penetrating keratoplasty were obtained via a materials transfer agreement from Nottingham University Hospitals Trust. All human tissue work was performed in strict accordance with the UK Human Tissue Act. Human corneal stromal cells (CSCs) were extracted from corneoscleral rims using modified techniques previously described (Sidney et al., 2015). Briefly, the residual sclera was removed from the corneoscleral rim, and the remaining tissue was divided in approximately 16 pieces and placed into a 1 mg/mL collagenase solution (Sigma-Aldrich, UK). The tissue was then incubated under agitation at 37 °C for 7 h. After incubation the solution was filtered through a 40 µm cell strainer to remove cell debris and centrifuged at 200 x g for 5 min (Universal 32R, Hettich-Zentrifugen, Germany). The resulting cell pellet was cultured in M199 basal medium containing 20 % (v/v) fetal bovine serum (FBS, Sigma Aldrich, UK), 2 mM l-Glutamine (Sigma Aldrich, UK), and an antibiotic-antimycotic solution (AbAm). Cells were maintained at 37 °C in a humidified atmosphere with 5 % CO₂, with medium changes every 2–3 days. At 90 % confluence, cells were passaged using TryPLE express (Life Technologies, UK).

2.2. Parasite strain and growth conditions

2.2.1. *Acanthamoeba castellanii* culture

A. castellanii trophozoites of the T4 genotype were maintained in T-75 cm² tissue culture plastic flasks at a density of 1×10^6 trophozoites per flask. The trophozoites were axenically cultured in PYG growth

medium, which contained proteose peptone (0.75% w/v, Sigma-Aldrich, Germany), yeast extract (0.75% w/v, Sigma-Aldrich, USA), and glucose (1.5% w/v, Sigma-Aldrich, Germany), as described previously (Khan et al., 2001; Ortega-Rivas et al., 2016). The culture flasks were incubated in a humidified atmosphere at 25 °C, and PYG medium was changed twice a week. The PYG medium was renewed the day prior to each experiment to promote the growth of active trophozoites.

2.2.2. Preparation of the conditioned medium (ACCM)

Following 24 h of seeding at a density of 1×10^6 trophozoites per flask as illustrated above, *A. castellanii* trophozoites, routinely maintained in PYG medium, were adapted to grow in the culture medium of corneal cells (M199 for CSCs or EpiLife™ for ihCECs). This adaptation was achieved by incubating *A. castellanii* in the corresponding medium for 48 h prior to experimental use. Subsequently, *A. castellanii* trophozoites were separated from the culture medium by centrifugation at 1000 x g (Allegra X-22R centrifuge, Beckman Coulter™) for 5 min. The pellet was discarded, and the supernatant was filtered through a 0.2 µm filter. Different dilutions of the filtered supernatant (hereafter referred to as *Acanthamoeba castellanii*-derived conditioned medium [ACCM]) were prepared by mixing the ACCM with M199 or EpiLife™ in various volumes (v/v) of 25 %, 50 %, 75 %, and 100 %. These were then used to test the cytotoxic effect of ACCM on corneal cells as described below.

2.2.3. Bicinchoninic acid assay (BCA)

The BCA protein assay was used to quantify the protein concentration of ACCM (including M199 and EpiLife™). The assay was performed according to the manufacturer's instructions, using bovine serum albumin (BSA) as a standard (Thermo Scientific Pierce, USA). Briefly, 25 µL of each sample was added in triplicate to a 96-well microplate, followed by the addition of 200 µL of BCA working reagent per well. The plate was shaken for 30 s and then incubated for 30 min at 37 °C. Absorbance was measured at 562 nm using a microplate reader (BMG Labtech GmbH, Offenburg, Germany).

2.3. Viability assays

The cytotoxic effect of ACCM on the viability of CSCs and ihCECs was examined using three assays: alamarBlue®, MTT, and Sulforhodamine B (SRB). Each assay was performed in triplicate in 96-well flat bottom microplates (Costar; Corning, USA) under aseptic conditions in a laminar flow hood. Cells were seeded in 96-well plates at a density of 1×10^4 cells/well for ihCECs and at 6×10^3 cells/well for CSCs, with 0.1 mL of the respective culture medium per well. Cell numbers were determined using a hemocytometer. After 48 h of attachment, the media in each well was replaced with ACCM at concentrations of 25 %, 50 %, 75 %, and 100 %, bringing the final volume to 100 µL medium per well. Untreated wells contained 100 µL of M199 for CSCs and EpiLife™ for ihCECs. The plates were incubated at 37 °C and analyzed after 3, 24 and 48 h using the alamarBlue®, MTT and SRB assays as detailed below.

2.3.1. Evaluation of metabolic activity using alamarBlue® assay

Cell viability was examined by addition 10 µL of alamarBlue® (Thermo-Fisher Scientific, USA) per well, as described previously (Larson et al., 1997). The plates were incubated for 1 h, and absorbance was measured at 492 nm using a microplate reader (Labtech International Ltd, LT- 4000, UK) at 3, 24 and 48 h post-incubation.

2.3.2. MTT cell viability assay

Cell viability was determined via the addition of 10µL/well of MTT, [3-(4,5-dimethyl-2-thiazolyl)-2,5-diphenyl-2H-tetrazolium bromide] (5 mg/mL in phosphate-buffered saline [PBS]; Sigma, USA) to each well for 4 h at 37 °C and 5 % CO₂. Subsequently, 100 µL of MTT solubilization solution (10 % SDS in 0.01 M HCl) was added to each well, and the plate was incubated for an additional 1 h at 37 °C. The number of living cells, directly correlated to the amount of reduced MTT, was quantified by

measuring absorbance at 570 nm using a microplate reader (Labtech International Ltd, LT- 4000, UK).

2.3.3. Sulforhodamine B assay

At 3, 24 and 48 h after incubation with ACCM, the samples were fixed and subsequently stained using the SRB assay as described previously (Ortega-Rivas et al., 2016; Vichai and Kirtikara, 2006). Briefly, the samples were fixed with 25 μ L of cold (10 %, 4 °C) trichloroacetic acid (TCA, Fisher, Belgium) per well, and incubated at 4 °C for 1 h. TCA was then discarded, and the plates were washed with distilled water and allowed to dry at ambient temperature. Next, 25 μ L of SRB solution (0.05 % SRB dye in 1 % acetic acid) was added to each well to stain the cells. The plates were covered with aluminum foil to shield them from light and left for 15 min at ambient temperature. The samples were then washed three-times with 1 % (v/v) acetic acid to remove excess unbound SRB dye. The plates were air-dried before adding 150 μ L of 10 mM Tris-base (tris(hydroxymethyl)aminomethane, pH 10.5) to each well to solubilize the SRB dye. The plates were placed on a shaker for 5 min to ensure even distribution of the dye in the well's supernatant. The absorbance was measured at 492 nm using a microplate reader (Labtech International Ltd, LT- 4000, UK).

2.4. In vitro cell toxicity studies

2.4.1. Lactate dehydrogenase (LDH) cytotoxicity assay

The cytotoxicity of ACCM against ihCECs and CSCs was assessed using the LDH cytotoxicity assay according to the manufacturer's instructions (Pierce™ LDH cytotoxicity assay kit; Thermo Scientific, USA). Briefly, ihCECs and CSCs were seeded in 96-well plates at 5×10^3 and 3×10^3 cells/well, respectively. Cells were allowed to attach for 24 h, after which the media was removed and replaced with media containing 50 % of ACCM or left untreated (control). At 3, 24 and 48 h post-exposure to ACCM, 50 μ L of culture supernatant per well was collected and transferred into another 96-well plate in triplicate. Then, 50 μ L of reaction mix solution containing substrate was added per well, mixed by gentle pipetting, and the plate was incubated for 30 min at ambient temperature, protected from light. After the addition 50 μ L of stop solution, the absorbance was measured at 490 with 680 nm corrective background reading using a microplate reader (BMG Labtech GmbH, Offenburg, Germany).

2.4.2. Caspase 3 assay

Caspase-3 activity levels in CSCs and ihCECs was measured using the caspase-3 assay kit (Caspase-Glo® 3/7 assay kit; Promega, USA) according to the manufacturer's directions. Briefly, CSCs and ihCECs were seeded in 96-well plates at a density of 5×10^3 and 3×10^3 cells, respectively, and allowed to attach for 24 h. Subsequently, 50 % ACCM was added, and the cells were incubated for 3, 24 and 48 h at 37 °C. After incubation, 100 μ L of Caspase-Glo® 3/7 reagent was added to each well (control and treated groups with 50 % ACCM). The plates were covered and shaken for 30 s, then incubated for 30 min at ambient temperature. Luminescence was measured at 545–50 nm using a microplate reader (BMG Labtech GmbH, Offenburg, Germany).

2.5. Immunofluorescent staining of actin

CSCs or ihCECs were seeded in 24-well plates at 12×10^3 and 20×10^3 cells, respectively, and incubated with ACCM (M199 or EpiLife™) at various concentrations (100 %, 75 %, 50 % and 25 %) for 3, 24 and 48 h at 37 °C. The experiment was carried out at ambient temperature following the protocol described by Sidney et al. (2015). Briefly, the cells were fixed in 10 % buffered formalin (VWR, N. 9713.5000) for 10 min, and then washed three times with PBS. Cells were permeabilized with 0.1 % (v/v) Triton X-100 (Sigma Aldrich, UK) in PBS for 10 min. After three PBS washes, blocking buffer (1 % (v:v) BSA and 0.3 mol/L glycine in PBS; Sigma Aldrich) was added to the wells and incubated for

30 min. Samples were stained for F-actin with Alexa-Fluor 488 phalloidin (Life Technologies, 1:60 diluted in blocking buffer) for 20 min in the dark, followed by a single wash in blocking buffer. Cells were counterstained with DAPI (Life Technologies, 5 μ L/5 mL in blocking buffer) to stain the nuclei for 10 min. Images were obtained using an inverted wide-field fluorescence microscope (DM-IRB, Leica, Wetzlar, Germany) equipped with a Hamamatsu digital camera (Hamamatsu Photonics, Hamamatsu, Japan).

2.6. Transmission electron microscopy (TEM)

TEM was employed to investigate the ultrastructural alterations at the single-cell level post-ACCM treatment. CSCs and ihCECs were seeded in T-25 flasks at densified 7×10^4 and 12×10^4 cells, respectively for 48 h. Subsequently, 50 % ACCM was added, and the cells were incubated at 37 °C for another of 48 h. Following a previously established protocol (Maradze et al., 2018), cells were gently detached from the flasks using a cell scraper (Greiner, Bio-One, Germany) and fixed in 3 % glutaraldehyde in 0.1 M cacodylate buffer (TAAB Reading, UK) at 4 °C for 24 h. After fixation, cells were washed twice with cacodylate buffer and stored in cacodylate wash buffer at 4 °C for 24 h. Post-fixation was performed using 1 % osmium tetroxide (TAAB Reading, UK) at 4 °C for 1 h, followed by two washes in distilled water. Cells were then embedded in 3 % (w/v) agarose and dehydrated using an ascending ethanol series (50 %, 70 %, 90 %, and 100 % ethanol, twice for 10 min each), followed by dehydration with 100 % propylene oxide (propox) twice for 15 min each. After dehydration, cells were infiltrated with resin (1:3 resin mixed for 1 h, 1:1 resin mixed for 24 h) and embedded in plastic capsules in 100 % resin, then incubated at 60 °C for 48 h. Ultrathin sections (90 nm thickness) were cut using a Leica EM-UC6 ultramicrotome (Leica EM UC6, Germany), placed on gilder copper TEM grids (TAAB Reading, UK). The samples were stained with uranyl acetate solution followed by Reynolds' lead citrate (TAAB, UK) for 10 min each. Images were acquired using the Tecnai BioTwin-12 TEM (FEI, United States).

2.7. Protease inhibitor assay

A protease inhibitor cocktail (Sigma-Aldrich, UK) was added to ACCM (M199 and EpiLife media) at concentrations of 2.5, 5 and 10 μ L/mL and incubated for 30 min at 25 °C. Then, 100 μ L of treated ACCM were added to CSCs or ihCECs seeded in 96-well plates, which were incubated for 3, 6, 24 and 48 h at 37 °C and 5 % CO₂. Cells incubated in untreated medium or with 100 % ACCM were used as negative and positive controls, respectively. The proliferation rate of all cells subjected to different concentrations of the protease inhibitor and the control (untreated) cells was determined using the SRB assay as described above.

2.8. Statistical analysis

All statistical analysis was performed using GraphPad Prism version 7 (GraphPad, San Diego, CA, United States). Differences between the effect of ACCM at different treatment durations was determined by one-way analysis of variance (ANOVA) followed by Tukey's multiple comparison test or two-way ANOVA followed by the Dunnett's test, as indicated. Each experiment was performed three times with a minimum of three technical replicates per-experiment. Data are expressed as mean \pm SD. Statistical significance is indicated in the figures by asterisks as follows: $p < 0.05$ (*), $p < 0.01$ (**), $p < 0.001$ (***), and $p < 0.0001$ (****).

3. Results

3.1. Concentrations of protein in the ACCM

The BCA protein assay revealed that ACCM_M199 and ACCM_Epilife

had lower protein concentrations compared to the normal culture media (M199 and Epilife), which exhibited the highest protein concentrations. As shown in Table 1, increasing the concentration of the conditioned medium resulted in a decrease in protein concentration, suggesting an inverse correlation between the percentage of ACCM and protein concentration. This reduction in protein content at higher concentrations of ACCM_M199 and ACCM_Epilife is likely due to the activity of *A. castellanii* proteases degrading the proteins (Ramírez-Rico et al., 2015).

3.2. The effects of ACCM on corneal cell viability

The effects of ACCM on the viability and proliferation of CSCs and ihCECs were assessed using alamarBlue®, MTT, and SRB assays. Exposure to ACCM_M199 or ACCM_Epilife resulted in a dose-dependent decline in the viability and proliferation of CSCs and ihCECs at 3, 24 and 48 h of incubation for all assays (Figs. 1-2). The alamarBlue® assay showed statistically significant differences in CSC viability between treated and control groups at all incubation times (Fig. 1). MTT test results also revealed significant differences in CSC proliferation between treated and control cells at all examined times (Fig. 1). Similarly, the SRB assay indicated significant differences in CSC proliferation between treated and control groups at all incubation times (Fig. 1). For ihCECs, the alamarBlue® assay showed no significant differences in viability between treated and control groups at 3 h; however, significant differences were observed at 24 and 48 h (Fig. 2). The MTT results demonstrated a significant reduction in ihCEC viability between treated and control cells at 3, 24 and 48 h (Fig. 2). The SRB confirmed significant differences in the proliferation rate between treated and control groups at 3, 24 and 48 h (Fig. 2, C).

3.3. The cytotoxic effects of ACCM on corneal cells

CSCs and ihCECs were exposed to 50 % ACCM and the release of LDH enzyme into the cell culture medium was quantified. Based on previous findings indicating the susceptibility of corneal cells to high concentrations of ACCM_M199 or ACCM_Epilife, 50 % ACCM_M199 or 50ACCMEpilife were selected for corneal cell treatment. The results revealed significant differences between treated and control cells, with a notable increase in LDH levels observed for CSCs at 3 h followed by a decrease at 24 h (Fig. 3). Similarly significant differences were observed for ihCECs at all time points post-treatment, with an initial increase at 3 h, followed by decreases at 24 and 48 h (Fig. 3). We also examined the apoptotic activity of 50 % ACCM_M199 or ACCM_Epilife by measuring caspase activity using the caspase Glo-3/7 assay. In CSCs, caspase 3 was activated after 24 h of stimulation with 50 % ACCM h, with further activation observed at 48 h (Fig. 4). Conversely, in ihCECs, a significant reduction in caspase 3 levels was observed in the cells treated with ACCM at 48 h (Fig. 4).

Table 1

Protein concentrations in *A. castellanii*-conditioned medium (ACCM) ACCM_M199 and ACCM_Epilife, at concentrations of 100 %, 50 %, 25 % and 0 %, compared to control media.

Concentrations	Protein Concentration (µg/mL) *	
	ACCM_M199 (Mean ± SD)	ACCM_Epilife (Mean ± SD)
100 %	366.08 ± 16.71	238.42 ± 9.53
50 %	371.52 ± 5.81	257.41 ± 6.68
25 %	434.39 ± 18.38	289.54 ± 11.91
Control**	472.66 ± 17.23	303.21 ± 12.74

* Protein level was quantified using the BCA protein assay and the absorbance was measured at 562 nm. The experiment was performed three times with four technical replicates per-experiment.

**Normal M199 and Epilife medium without any contribution from *A. castellanii* secretome.

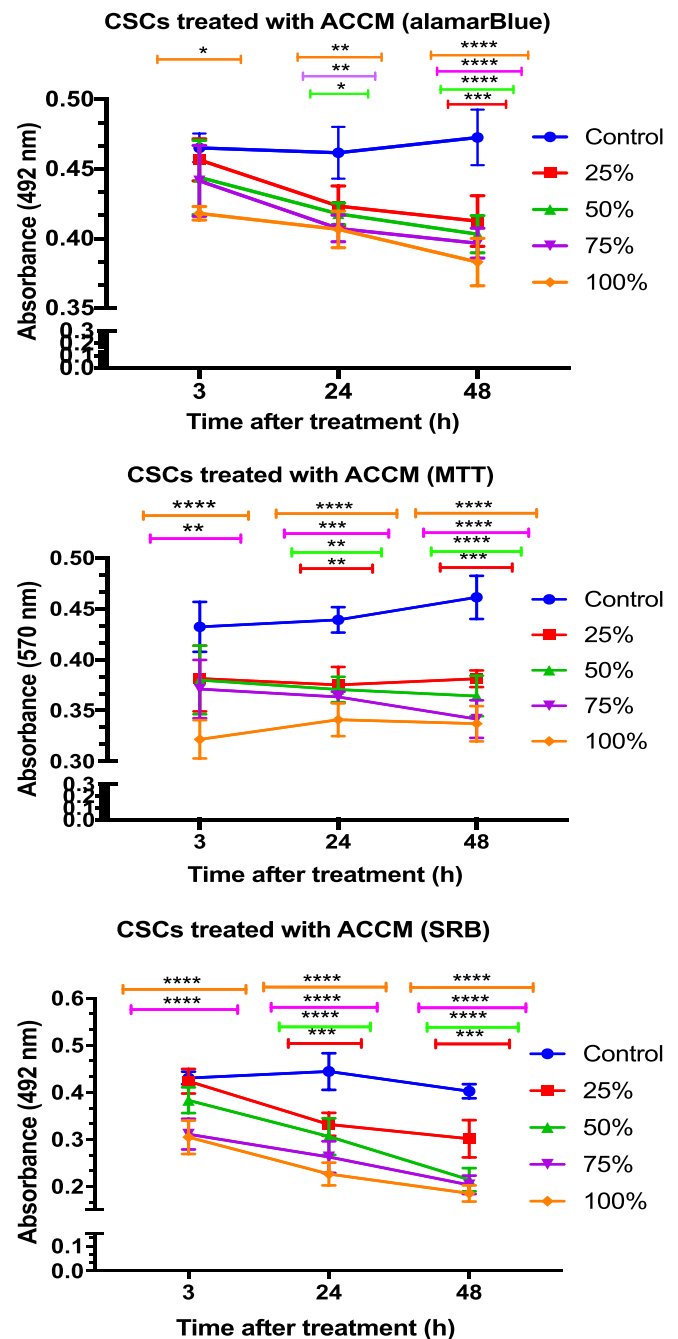


Fig. 1. Effect of ACCM on the viability and proliferation of CSCs assessed using alamarBlue®, MTT and SRB assays. CSCs were exposed to various concentrations of ACCM_M199 (25 %, 50 %, 75 %, and 100 %) at 37 °C for 3, 24 and 48 h. Cells treated with unconditioned M199 medium served as the control. Absorbance values are presented as means ± standard deviations (SDs) of four technical replicates, with each experiment repeated three times. Significant differences between ACCM-treated and untreated groups were detected using two-way ANOVA followed by Dunnett’s posttest. Statistical significance compared to the control is denoted as follows: *****p* < 0.0001; ****p* < 0.001; ***p* < 0.01; **p* < 0.05.

3.4. Actin cytoskeleton derangement

CSCs and ihCECs were subjected to phalloidin and DAPI staining to assess morphological alterations in actin arrangement following exposure to various concentrations of 50 % ACCM_M199 or 50 % ACCM_Epilife for different durations. As shown in (Fig. 5) for CSCs and ihCECs, the density of the cell monolayer was higher in the control compared to

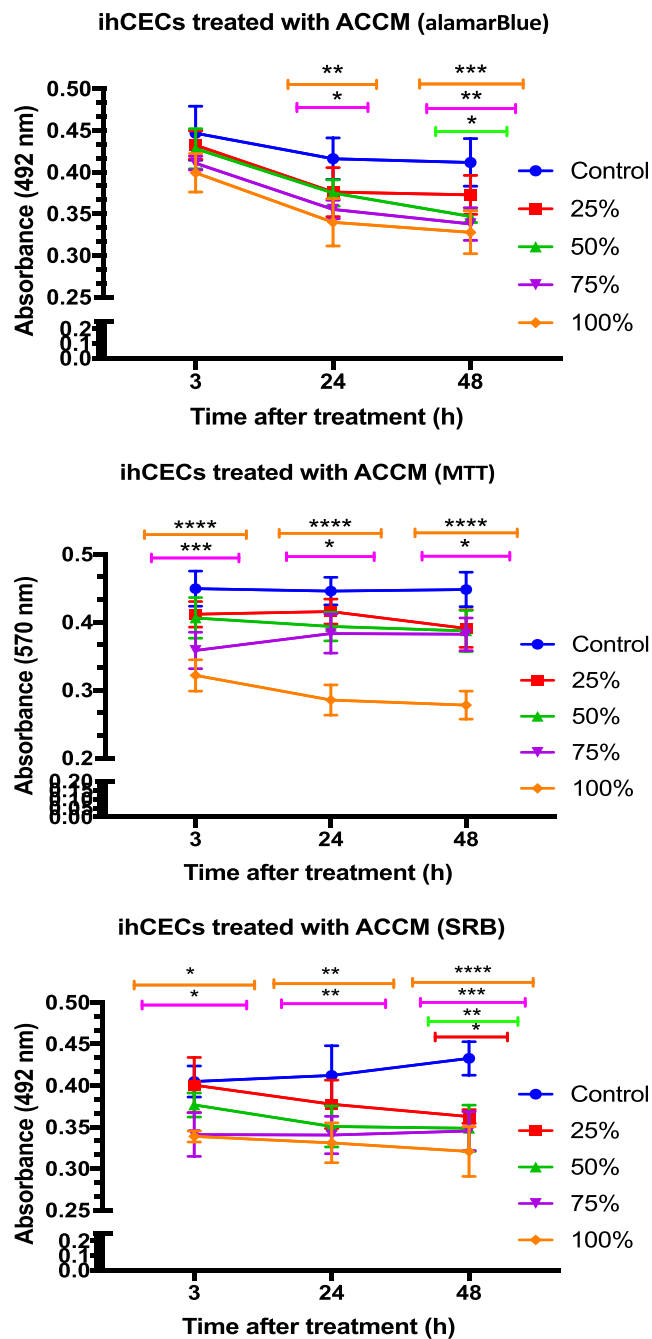


Fig. 2. Effect of ACCM on the viability and proliferation of ihCECs assessed using alamarBlue®, MTT and SRB assays. ihCECs were exposed to various concentrations of ACCM_Epilife (25 %, 50 %, 75 %, and 100 %) for 3, 24 and 48 h at 37 °C. Cells treated with unconditioned Epilife™ medium served as the control. Data are presented as absorbance values relative to untreated (control) cells. Significant differences between ACCM-treated and untreated cells were determined using two-way ANOVA followed by Dunnett’s posttest. Each experiment was performed three times with four technical replicates per-experiment. Statistical significance compared to the control is indicated as follows:**** $p < 0.0001$; *** $p < 0.001$; ** $p < 0.01$; * $p < 0.05$.

treated cells, with the integrity of the cell monolayer compromised in a dose-response manner. We also observed changes in the shape of CSCs and ihCECs, along with derangement of the actin cytoskeleton, were observed, particularly at higher concentrations and longer exposure times (i.e. at 24 and 48 h with 50 %, 75 % and 100 % ACCM). Additionally, ihCECs cultured with 50 %, 75 % and 100 % ACCM exhibited a transition to smaller, more rounded cells at 3, 24, and 48 h post exposure

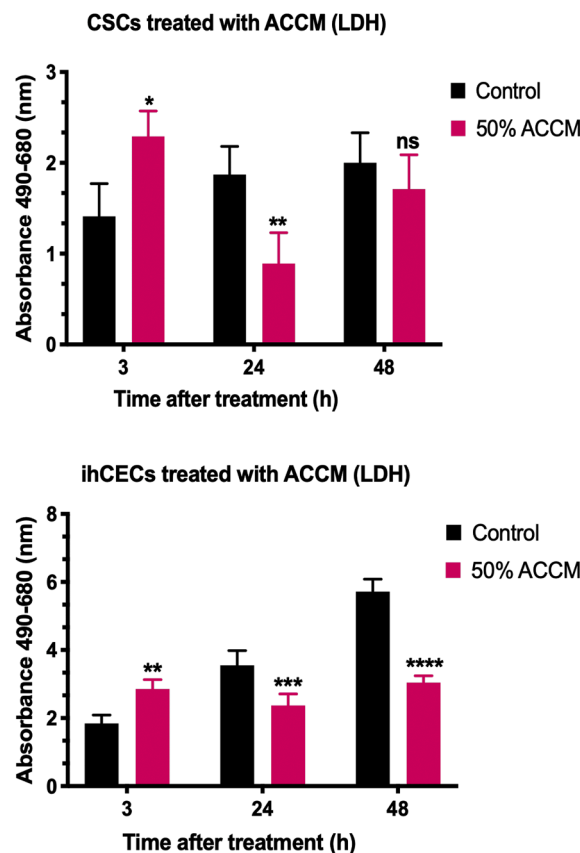


Fig. 3. Results of the cytotoxicity assessment using the LDH assay. CSCs and ihCECs were treated with 50 % of either ACCM_M199 or ACCM_Epilife for 3, 24 and 48 h at 37 °C. Absorbance was measured at 490 and 680 nm. Cells treated with unconditioned medium (M199 or Epilife™) served as controls. The experiment was replicated at least three times, with four technical replicates per experiment. Data are presented as the mean ± standard deviation (SD). One-way ANOVA Tukey’s multiple comparison test revealed significant differences between ACCM-treated and untreated cells. Statistical significance compared to the control is indicated as follows: **** $p < 0.0001$; *** $p < 0.001$; ** $p < 0.01$; * $p < 0.05$.

(Fig. 5). Manual cell counts conducted on the images presented in Fig. 5 revealed a significant decrease in the cell density, in a time- and concentration-dependent manner, for both cell types (Fig. 6).

3.5. TEM analysis of ACCM-treated corneal cells

To further elucidate the effects of 50 % ACCM_M199 or ACCM_Epilife on CSCs and ihCECs, TEM was performed to reveal the ultrastructural changes upon 50 % ACCM treatment for 48 h. Cells exhibited normal cellular components in untreated cultures of CSCs (Fig. 7A-D) and ihCECs (Fig. 8A-D), including intact nuclei, prominent nucleolus, normal cellular organelles, vacuoles, intact plasma membrane, with no sign of cellular or organelle damage. On the contrary, cells treated with 50 % ACCM for 48 h showed clear damages and morphological changes. The nucleus was less visible or even absent in some cells (Fig. 7E-H). Consistent with the findings in of CSCs, significant cellular damages and increased vacuolation were also observed in ihCECs compared to untreated cells (Fig. 8E-H).

3.6. Protective effects of enzyme inhibitor cocktail on ACCM cytotoxicity

We investigated whether the adverse effect of 50 % ACCM_M199 or ACCM_Epilife was attributable to the presence of proteases secreted by *A. castellanii* (Fig. 9). In CSCs, a gradual, dose-dependent increase in cell

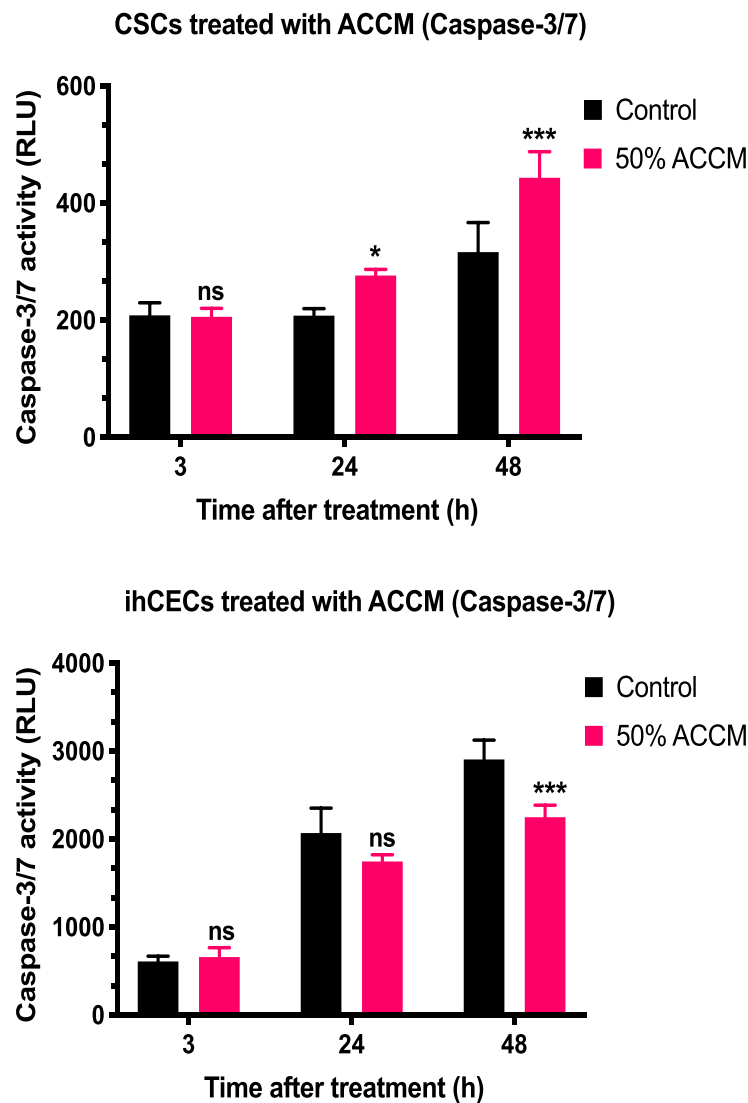


Fig. 4. Results of caspase activity in CSCs and ihCECs. Caspase 3/7 activity levels were assessed using recombinant human caspase-3 enzyme to evaluate the stimulatory or inhibitory effect of 50 % of ACCM_M199 or ACCM_Epilife at 3, 24 and 48 h at 37 °C. The bar chart depicts the means \pm standard deviations (SDs) of four technical replicates, with each experiment independently repeated three times. Data are presented as relative luminescence units (RLU), which correlate with caspase 3 activity. One-way ANOVA Tukey's multiple comparison test identified significant differences between cells treated with 50 % ACCM and untreated cells. Statistical significance compared to the control is indicated as follows: *** $p < 0.001$; ** $p < 0.01$; * $p < 0.05$.

proliferation was evident when treated with the protease inhibitor at all concentrations compared to untreated (control) cells at 3, 6, 24 and 48 h after incubation (Fig. 9). There were significant differences in CSC proliferation between the treated groups compared to the control at 24 and 48 h, suggesting the protective effect of the protease inhibitor cocktail against ACCM-induced damage. Similarly, the growth rate of treated ihCECs appeared to be maintained in the presence of protease inhibition, with significant differences observed between the treated groups and the control at 6, 24, and 48 h.

4. Discussion

Cellular damage from *A. castellanii* infection stems from its secreted molecules. The toxic effect of *A. castellanii* secretome has been evidenced across various cell types (Mattana et al., 1997, 2002). However, the exact role of cytolytic components within *A. castellanii* secretome in corneal infection remains incompletely understood. In this study, we investigated the cellular mechanisms underlying corneal cell (CSCs and ihCECs) vulnerability to ACCM's cytotoxicity. Our findings are consistent with previous studies (Mattana et al., 2002; Khan et al., 2000,

1997), showing that *A. castellanii* cytotoxicity against human ocular cells does not necessitate direct contact with the host cell; instead, damage can result from cell-free supernatant obtained from trophozoite cultures.

The influence of ACCM on CSCs and ihCECs viability and proliferation, evaluated through alamarBlue, MTT and SRB assays, exhibited a marked decrease in both parameters (Figs. 1 and 2). This suggests that ACCM exposure adversely affects the viability and growth kinetics of corneal cells. Examining the ACCM's cytotoxicity against these cells involved the LDH assay. LDH, an enzyme released from the damaged cell membranes into the culture medium, serves as a reliable marker for cytotoxicity and cell death (Parhamifar, Andersen and Moghimi, 2019; Kumar, Nagarajan and Uchil, 2018). In our study, LDH enzyme levels in the culture medium were quantified. Elevated LDH levels post-ACCM treatment indicate membrane leakage, a response that appears to vary with cell type and exposure duration (Fig. 3). Interestingly, an initial increase in LDH levels was observed at 3 h, suggesting significant cell lysis in both CSCs and ihCECs, followed by a subsequent decline at 24 h in CSCs, and at 24 and 48 h in ihCECs.

We also investigated the changes in caspase-3 and caspase-7 activity. Previous research has suggested that changes in mitochondrial

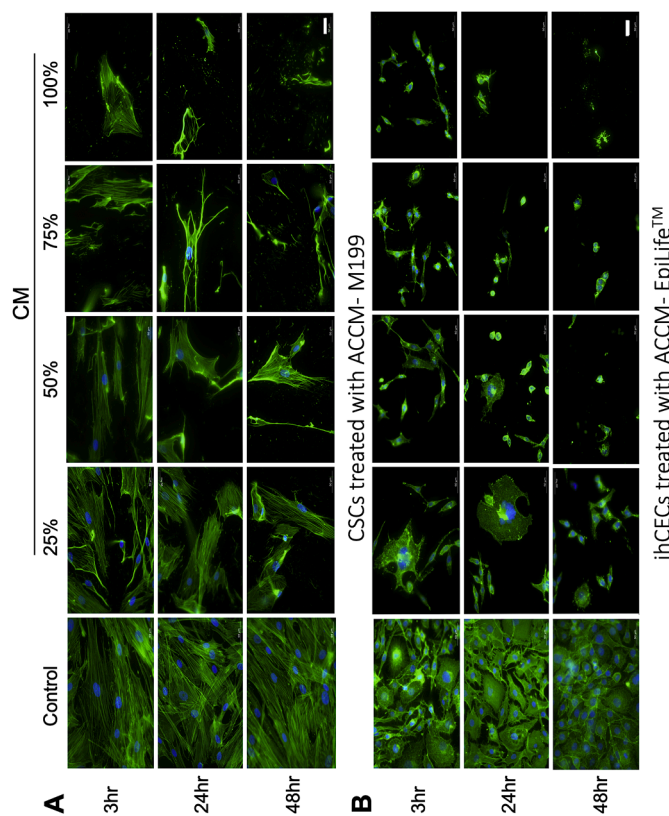


Fig. 5. Effect of ACCM on the actin cytoskeleton using fluorescence staining. (A) CSCs and (B) ihCECs were exposed to 50 % of ACCM_{M199} or 50 % ACCM_{Epilife}, at the specified concentrations and durations of incubation. Following fixation with 10 % formalin for 10 min, cells were stained for F-actin with Alexa Fluor 488 phalloidin, and nuclei were counterstained with DAPI. Images were captured using an inverted wide-field fluorescence microscope. Scale bar (25 μ m) applies to all images. The imaging showed a significant decrease in cells density and disruption of the cell actin cytoskeleton in a time- and concentration-dependent manner.

membrane integrity may lead to the release of cytochrome c in the cytoplasm, subsequently activating caspases (Liu et al., 1996), particularly caspase 3, which mediates mitochondrion-initiated apoptosis (Thornberry and Lazebnik, 1998). Therefore, we examined whether caspase 3 and caspase-7 were activated in both CSCs and ihCECs following ACCM treatment. Caspase activity in these cells was evaluated using a caspase-3/7 activity assay (Fig. 4). In CSCs, caspase-3/7 activation was evident after stimulation with 50 % ACCM for 24 h, and peaked at 48 h. Conversely, in ihCECs, a significant decrease in caspase level was observed after 48 h of ACCM treatment. The proapoptotic effect of ACCM on CSCs is consistent with previous research (Mattana et al., 2002), suggesting that *A. castellanii* induces cell death through the release of adenosine diphosphate and other metabolites within the secretion of proinflammatory cytokines, leading to apoptosis. However, our results revealed significant reduction in caspase activity compared to the ihCECs control, potentially indicating an anti-apoptotic effect or possibly linked to a decreased cell number in treated cells due to lysis. The cell line exhibits a lot of natural turnover and apoptosis, leading to both LDH and caspase production in the control. This effect would be less pronounced if there were fewer cells due to the cytotoxicity of the treatment.

Disruption of the actin cytoskeleton represents a pathological hallmark of cell damage, because this structure plays a critical role in maintaining cellular architecture, function and adhesion (Soto-Arredondo et al., 2014). In our study, we examined the effect of ACCM on actin cytoskeleton arrangements by investigating the structural changes

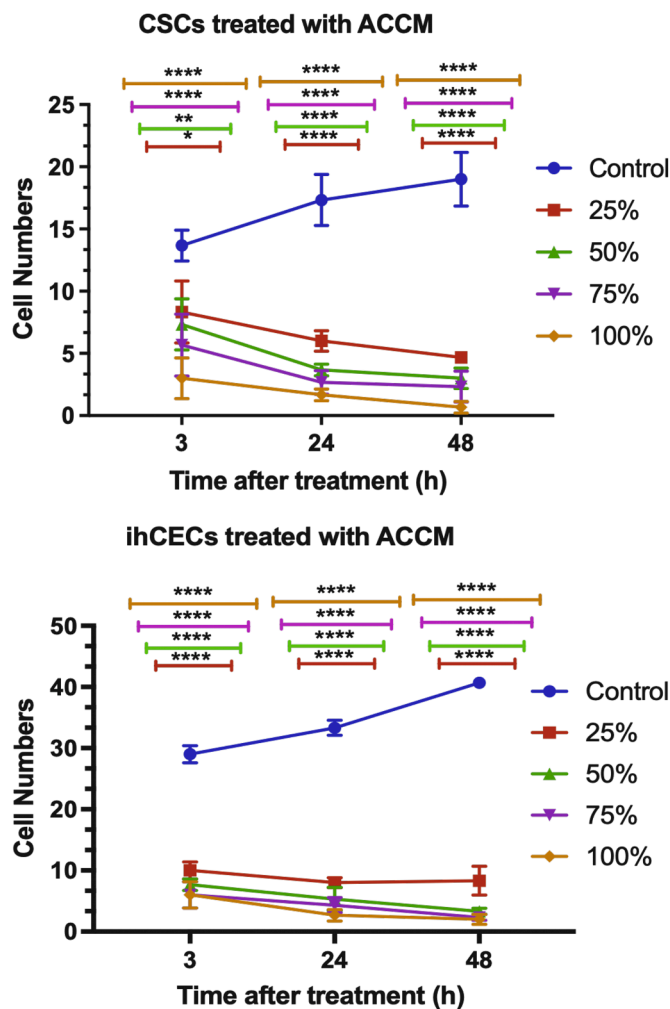


Fig. 6. Influence of ACCM on the cell density of CSCs and ihCECs. The cell counting was conducted manually for each cell line. Each experiment was performed three times with three technical replicates per-experiment. Data are presented as the means \pm standard deviations (SDs). Two-way ANOVA followed by Dunnett's posttest identified significant differences between cells treated with various concentrations and controls. Statistical significance compared to the control is denoted by asterisks: **** p < 0.0001; *** p < 0.001; ** p < 0.01; * p < 0.05.

in cultured CSCs and ihCECs treated with varying doses of ACCM for 3, 24 and 48 h (Fig. 5). Lower concentrations induced mild derangement of the actin cytoskeleton, while higher concentrations and longer treatment durations exacerbated this derangement, resulting in cell deformation. The cytotoxic effects of ACCM were more pronounced in ihCECs compared to CSCs, with the most significant damage observed after 24 h of incubation, leading to extensive cellular damage and rounding. Actin fibers not only contribute to the maintenance of cellular structure but also facilitate *A. castellanii* adhesion to host cells (Soto-Arredondo et al., 2014) and potentially engage in interactions with various structural molecules. Therefore, it is sensible to anticipate that ACCM-induced disruption of the actin cytoskeleton can profoundly affect the integrity, function and survival of host cells.

Further evidence supporting the adverse impact of ACCM on corneal cells was achieved by ultrastructural microscopic analysis (Figs. 7,8). Treated cells showed significant damage and irregularities, accompanied by apparent leakage of intracellular contents. Consistent with preceding findings, evidence of apoptosis and cell lysis was observed in treated cells, suggesting that ACCM likely triggers cell death through these mechanisms in host cells. Similar observations have been reported

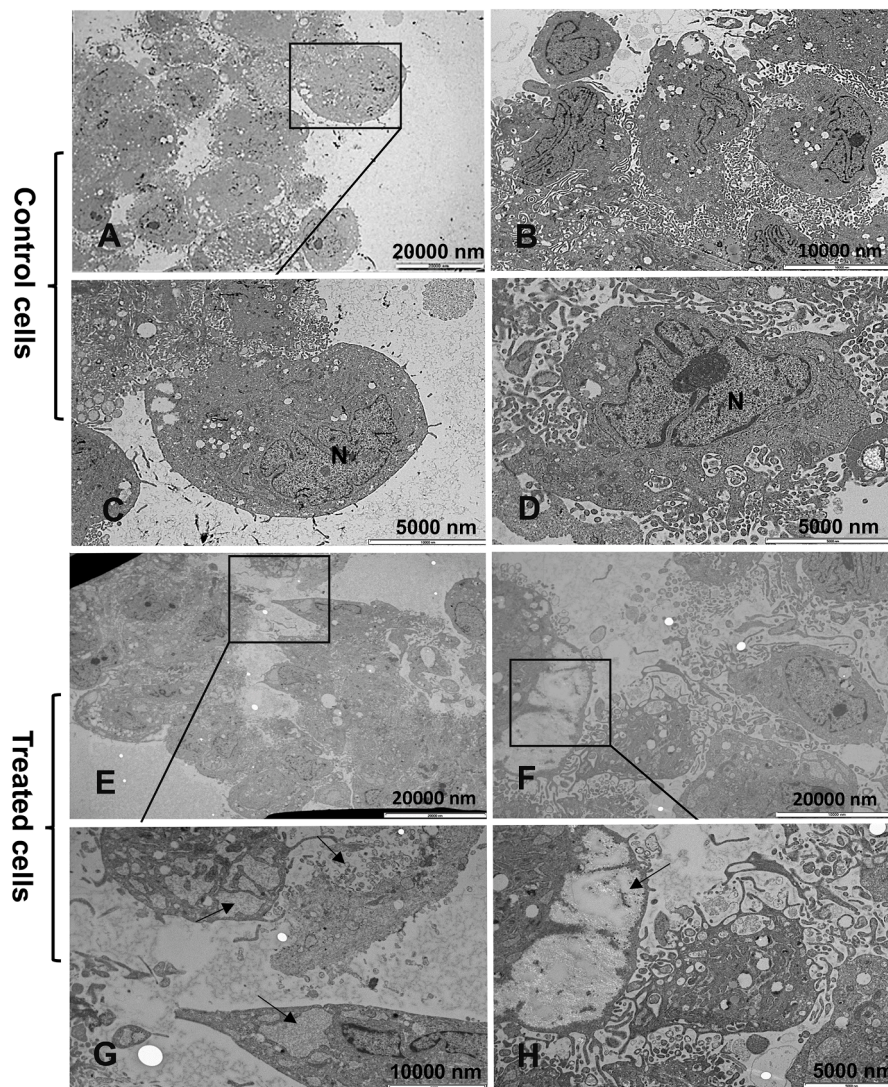


Fig. 7. Ultrastructural changes in CSCs following treatment with 50 % ACCM–M199 for 48 h. (A–D) Control CSCs exhibited normal morphology with a intact nucleus (N) and prominent nucleolus. (E–H) CSCs treated with ACCM showed damages and morphological changes (arrows), indicating cell death characterized by the absence of a discernible nucleus, presence of cytoplasmic vesicles, and depletion of cellular organelles (arrows).

previously (Pettit et al., 1996; González-Robles et al., 2006), however cell damage was attributed to direct physical contact with *A. castellanii* trophozoites.

Proteases in protozoan organisms are recognized for their dual roles in host tissue destruction, pathogenesis, and digestion of phagocytosed food (Klemba and Goldberg, 2002; Heredero-Bermejo et al., 2015). Within *A. castellanii*, proteases serve as virulence factors (Kim et al., 2006; Serrano-Luna et al., 2006), contribute to the encystation process (Moon et al., 2008), and facilitate adhesion (Singh et al., 2012). Studies utilizing proteinase inhibitors have demonstrated the essential role of protease activity in the development of focal lesions in HeLa cells (Heredero-Bermejo et al., 2015), and corneal endothelial cells (Khan et al., 2000). These studies have further identified the predominant presence of cysteine and serine proteases in amoeba extracts. In our study, we neutralized the enzymatic activities in ACCM using a protease inhibitor cocktail with broad specificity against serine, cysteine, aspartic, and aminopeptidases (Fig. 9). By inhibiting the enzymatic activities in ACCM using this protease inhibitor cocktail, we reaffirmed previous findings indicating that *A. castellanii* expresses proteases, which crucial for the pathogenesis of *A. castellanii* infection.

The results presented here showed that ACCM induces a detrimental effect on both types of corneal cells, with the ultrastructural alterations

in ihCECs being markedly more severe compared to CSCs. This discrepancy in cell sensitivity can largely be attributed to variations in cell-specific functions that influence their response to ACCM. CSCs, being primary cells, are expected to exhibit differences in metabolic activity, natural antioxidant activity, and proliferative capacity compared to ihCECs, which are a cell line. Primary cells generally maintain a better apoptotic balance and more stable metabolism compared to cell lines (Joris et al., 2013). Consistent with this notion, our study reveal that CSCs consistently exhibit reliable results across most experiments, whereas ihCECs exhibit some variability, particularly when cultured in large plates and flasks, where their growth appears slow and they are more susceptible to ACCM's effects. Considering these findings and given that primary cells offer a more physiologically relevant model compared to cell lines, CSCs provide a more suitable system for evaluating ACCM cytotoxicity.

The distinct characteristics of stromal cells and corneal epithelial cells result in varied interaction profiles with *A. castellanii*. During *Acanthamoeba* infection in corneal stromal cells, a series of sequential changes occur, commencing with the production of pathogenic proteases that degrade the extracellular matrix, leading to cytolysis and apoptosis (Marciano-Cabral and Cabral, 2003). These alterations ultimately lead to the breakdown of collagen surrounding corneal stromal

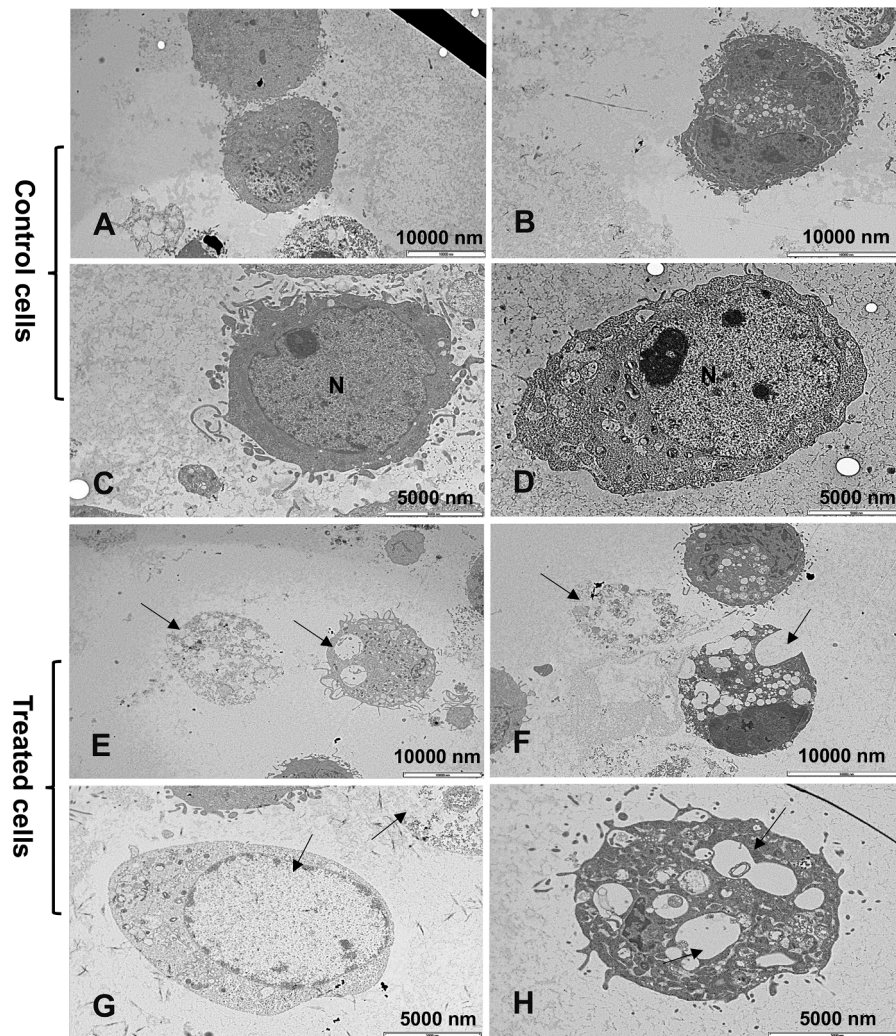


Fig. 8. Ultrastructural changes in ihCECs following treatment with 50 % ACCM-Epilife™ for 48 h. (A-D) Control ihCECs appeared morphologically normal with a intact nucleus (N) and conspicuous nucleolus. (E-H) ihCECs treated with ACCM showed damages and morphological changes (arrows), with some cells appeared dead, lacking a nucleus, and showing depletion of cellular organelles (arrows).

cells. Given that the human corneal epithelium harbors dendritic cells, impairment of these cells becomes a prerequisite for AK (Alzubaidi et al., 2016).

The BCA protein assay revealed a reduced protein concentration in ACCM_M199 and ACCM_Epilife, correlating with respective percentages (100 %, 50 %, and 25 %) of ACCM analyzed, compared to the baseline protein concentration detected in normal culture medium (i.e., M199 and Epilife), which had the highest protein levels (Table 1). *A. castellanii* trophozoites exhibit metabolic activity, enabling their survival and replication outside host cells, as they are typically auxotrophic for many nutrients (Naemat et al., 2018; Schunder et al., 2014; Dolphin, 1976). Thus, the decrease in protein levels within the conditioned medium is expected. However, it remains interesting to investigate the impact of *A. castellanii* growth on the metabolic composition of the culture medium.

In summary, our study shows that cell-free supernatants from *A. castellanii* culture containing soluble factors, such as proteases, adversely affect the function and structure of CSCs and ihCECs. These effects manifest in compromised cell viability, reduced cell proliferation and cell death. The loss of cell viability and increased cell death correlated with disturbances in the actin cytoskeleton and marked ultrastructural alterations. Our research also revealed that inhibition of ACCM's proteolytic activity rescued cell proliferation, highlighting the role of proteases in *A. castellanii* virulence. By using specific protease

inhibitors to dissect the contributions of different protease classes namely serine, cysteine, and metalloproteinases, future investigations can reveal more insight into the proteolytic mechanisms underlying *A. castellanii* pathogenicity. By further elucidating the molecular mechanisms governing the cytotoxic activity of ACCM, we may pave the way for the development of interventions aimed at mitigating or preventing corneal injury in individuals afflicted with AK.

CRediT authorship contribution statement

Abdullah Alhazmi: Methodology, Investigation, Data curation, Writing – original draft. **Laura E. Sidney:** Supervision, Validation, Writing – review & editing. **Andy Hopkinson:** Supervision, Validation, Writing – review & editing. **Hany M. Elsheikha:** Conceptualization, Validation, Visualization, Supervision, Writing – review & editing.

Declaration of competing interest

The authors declare that they have no known competing financial interests or personal relationships that could have appeared to influence the work reported in this article

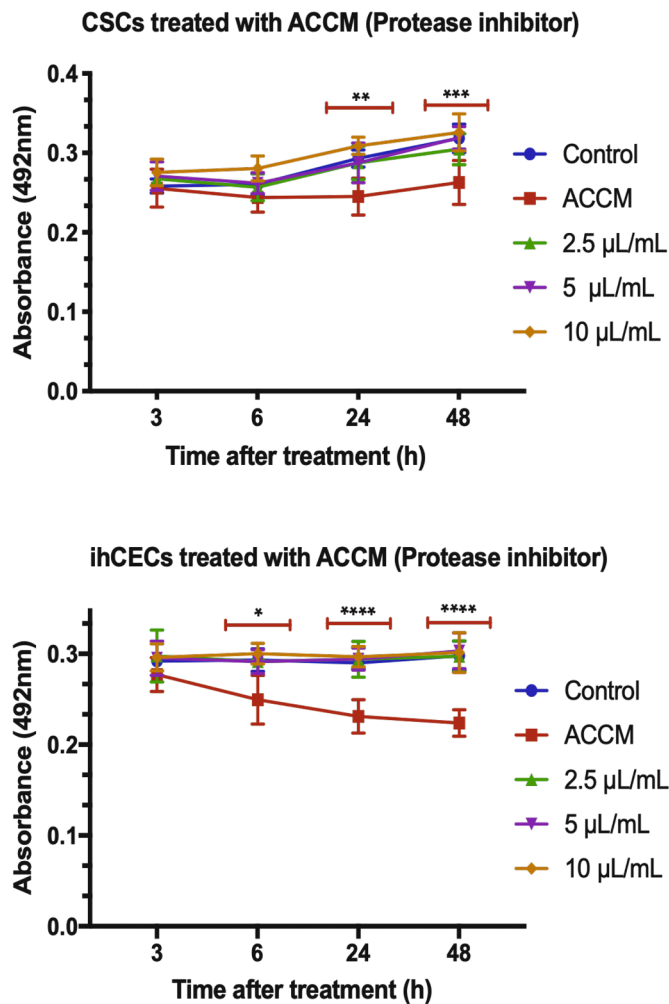


Fig. 9. Protease inhibitor cocktail protects CSCs and ihCECs from the cytotoxic effect of ACCM. CSCs and ihCECs were treated with 50 % of ACCM_M199 or ACCM_Epilife treated with a protease inhibitor cocktail at various concentrations (2.5, 5 and 10 $\mu\text{L}/\text{mL}$). Cells were then incubated for 3, 6, 24 and 48 h at 37 $^{\circ}\text{C}$, and cell proliferation was examined using the SRB assay. Absorbance data were measured at 492 nm. Two-way ANOVA followed by Dunnett's posttest identified significant differences between cells treated with ACCM and untreated (control) cells. Each experiment was performed three separate times, with four technical replicates each time. Statistical significance compared to the control is indicated as follows: **** $p < 0.0001$; *** $p < 0.001$; ** $p < 0.01$; * $p < 0.05$.

Data availability

Data will be made available on request.

Acknowledgments

We thank the University of Nottingham School of Life Sciences Imaging Unit (SLIM) for their contribution to this publication.

Funding

This work was supported by a scholarship from Umm Al Qura University, Ministry of Education of Saudi Arabia to A.A.

References

- Alzubaidi, R., Sharif, M.S., Qahwaji, R., Ipson, S., Brahma, A., 2016. In vivo confocal microscopic corneal images in health and disease with an emphasis on extracting features and visual signatures for corneal diseases: a review study. *Br. J. Ophthalmol.* 100 (1), 41–55.
- Araki-Sasaki, K., Ohashi, Y., Sasabe, T., Hayashi, K., Watanabe, H., Tano, Y., Handa, H., 1995. An SV40-immortalized human corneal epithelial cell line and its characterization. *Invest. Ophthalmol. Vis. Sci.* 36, 614–621.
- Cao, Z., Jefferson, D.M., Panjwani, N., 1998. Role of carbohydrate-mediated adherence in cytopathogenic mechanisms of *Acanthamoeba*. *J. Biol. Chem.* 273 (25), 15838–15845.
- Carnt, N., Hoffman, J.J.MBBS, Verma, S., Hau, S., Radford, C.F., Minassian, D.C., Dart, J. K.G., 2018. *Acanthamoeba* keratitis: confirmation of the UK outbreak and a prospective case-control study identifying contributing risk factors. *Br. J. Ophthalmol.* 102 (12), 1621–1628.
- Dolphin, W.D., 1976. Effect of glucose on glycine requirement of *Acanthamoeba castellanii*. *J. Protozool.* 23 (3), 455–457.
- Elsheikha, H.M., Siddiqui, R., Khan, N.A., 2020. Drug discovery against *Acanthamoeba* infections: present knowledge and unmet needs. *Pathogens*. 2020 9 (5), 405.
- Garate, M., Marchant, J., Cubillos, I., Cao, Z., Khan, N.A., Panjwani, N., 2006. In vitro pathogenicity of *Acanthamoeba* is associated with the expression of the mannose-binding protein. *Invest. Ophthalmol. Vis. Sci.* 47 (3), 1056–1062.
- González-Robles, A., Castañón, G., Cristóbal-Ramos, A., Lázaro-Haller, A., Omaña-Molina, M., Bonilla, P., Martínez-Palomo, A., 2006. *Acanthamoeba castellanii*: structural basis of the cytopathic mechanisms. *Exp. Parasitol.* 114 (3), 133–140.
- Herederer-Bermejo, I., Criado-Fornelio, A., De Fuentes, I., Soliveri, J., Copa-Patiño, J.L., Pérez-Serrano, J., 2015. Characterization of a human-pathogenic *Acanthamoeba griffini* isolated from a contact lens-wearing keratitis patient in Spain. *J. Parasitol.* 142 (2), 363–373.
- Jiang, C., Sun, X., Wang, Z., Zhang, Y., 2015. *Acanthamoeba* keratitis: clinical characteristics and management. *Ocul. Surf.* 13164–13168.
- Joo, S.Y., Aung, J.M., Shin, M., Moon, E.K., Kong, H.H., Goo, Y.K., Chung, D.I., Hong, Y., 2022. Sirtinol suppresses trophozoites proliferation and encystation of *Acanthamoeba* via inhibition of Sirtuin family protein. *Korean J. Parasitol.* 60 (1), 1–6.
- Joris, F., Manshian, B., Peynshaert, K., De Smedt, S.C., Braeckmans, K., Soenen, S.J., 2013. Assessing nanoparticle toxicity in cell-based assays: influence of cell culture parameters and optimized models for bridging the in vitro-in vivo gap. *Chem. Soc. Rev.* 42 (21), 8339–8359.
- Kalra, S.K., Sharma, P., Shyam, K., Tejan, N., Ghoshal, U., 2020. *Acanthamoeba* and its pathogenic role in granulomatous amebic encephalitis. *Exp. Parasitol.* 208, 107788.
- Khan, N., Jarroll, E., Paget, T., 2001. *Acanthamoeba* can be differentiated by the polymerase chain reaction and simple plating assays. *Curr. Microbiol.* 43, 204–208.
- Khan, N.A., Jarroll, E.L., Panjwani, N., Cao, Z., Paget, T.A., 2000. Proteases as markers for differentiation of pathogenic and nonpathogenic species of *Acanthamoeba*. *J. Clin. Microbiol.* 38 (8), 2858–2861.
- Kim, W.T., Kong, H.H., Ha, Y.R., Hong, Y.C., Jeong, H.J., Yu, H.S., Chung, D.I., 2006. Comparison of specific activity and cytopathic effects of purified 33 kDa serine proteinase from *Acanthamoeba* strains with different degree of virulence. *Korean J. Parasitol.* 44, 321–330.
- Klemba, M., Goldberg, D.E., 2002. Biological roles of proteases in parasitic protozoa. *Annu. Rev. Biochem.* 71 (1), 275–305.
- Köhler, M., Mrva, M., Walochnik, J., 2016. *Acanthamoeba*. *Molecular Parasitology*. Springer, pp. 285–324.
- Kumar, P., Nagarajan, A., Uchil, P.D., 2018. Analysis of cell viability by the lactate dehydrogenase assay. *Cold Spring Harb. Protoc.* 2018 (6), 465–468.
- Larson, E.M., Doughman, D.J., Gregerson, D.S., Obritsch, W.F., 1997. A new, simple, nonradioactive, nontoxic in vitro assay to monitor corneal endothelial cell viability. *Invest. Ophthalmol. Vis. Sci.* 38, 1929–1933.
- Leitsch, D., Köhler, M., Marchetti-Deschmann, M., Deutsch, A., Allmaier, G., Duchêne, M., Walochnik, J., 2010. Major role for cysteine proteases during the early phase of *Acanthamoeba castellanii* encystment. *Eukaryot. Cell* 9, 611–618.
- Liu, X., Kim, C.N., Yang, J., Jemmerson, R., Wang, X., 1996. Induction of apoptotic program in cell-free extracts: requirement for dATP and cytochrome c. *Cell* 86 (1), 147–157.
- Mahdavi Poor, B., Rashedi, J., Asgharzadeh, V., Mirmazhary, A., Gheitarani, N., 2023. Proteases of *Acanthamoeba*. *Parasitol. Res* 123 (1), 19.
- Maradze, D., Musson, D., Zheng, Y., Cornish, J., Lewis, M., Liu, Y., 2018. High magnesium corrosion rate has an effect on osteoclast and mesenchymal stem cell role during bone remodelling. *Sci. Rep.* 8 (1), 1–15.
- Marciano-Cabral, F., Cabral, G., 2003. *Acanthamoeba* spp. as agents of disease in humans. *Clin. Microbiol. Rev.* 16 (2), 273–307.
- Marciano-Cabral, F., Toney, D.M., 1998. The interaction of *Acanthamoeba* spp. with activated macrophages and with macrophage cell lines. *J. Eukaryot. Microbiol.* 45, 452–458.
- Mattana, A., Bennardini, F., Usai, S., Fiori, P.L., Franconi, F., Cappuccinelli, P., 1997. *Acanthamoeba castellanii* metabolites increase the intracellular calcium level and cause cytotoxicity in Wish cells. *Microb. Pathog.* 23, 85–93.
- Mattana, A., Cappai, V., Alberti, L., Serra, C., Fiori, P.L., Cappuccinelli, P., 2002. ADP and other metabolites released from *Acanthamoeba castellanii* lead to human monocytic cell death through apoptosis and stimulate the secretion of proinflammatory cytokines. *Infect. Immun.* 70 (8), 4424–4432.
- Mitra, M.M., Alizadeh, H., Gerard, R.D., Niederkorn, J.Y., 1995. Characterization of a plasminogen activator produced by *Acanthamoeba castellanii*. *Mol. Biochem. Parasitol.* 73 (1–2), 157–164.

- Moon, E.K., Chung, D.I., Hong, Y.C., Kong, H.H., 2008. Characterization of a serine proteinase mediating encystation of *Acanthamoeba*. *Eukaryot. Cell* 7 (9), 1513–1517.
- Moon, E.K., Hong, Y., Chung, D.I., Kong, H.H., 2012. Cysteine protease involving in autophagosomal degradation of mitochondria during encystation of *Acanthamoeba*. *Mol. Biochem. Parasitol.* 185, 121–126.
- Naemat, A., Sinjab, F., McDonald, A., Downes, A., Elfick, A., Elsheikha, H.M., Notingher, I., 2018. Visualizing the interaction of *Acanthamoeba castellanii* with human retinal epithelial cells by spontaneous Raman and CARS imaging. *J. Raman Spectrosc.* 49 (3), 412–423.
- Ortega-Rivas, A., Padrón, J., Valladares, B., Elsheikha, H., 2016. *Acanthamoeba castellanii*: a new high-throughput method for drug screening in vitro. *Acta Trop* 164, 95–99.
- Parhamifar, L., Andersen, H., Moghimi, S.M., 2019. Lactate dehydrogenase assay for assessment of polycation cytotoxicity. *Methods Mol. Biol.* 1943, 291–299.
- Pettit, D., Williamson, J., Cabral, G., Marciano-Cabral, F., 1996. In vitro destruction of nerve cell cultures by *Acanthamoeba* spp.: a transmission and scanning electron microscopy study. *J. Parasitol.* 82 (5), 769.
- Ramírez-Rico, G., Martínez-Castillo, M., de la Garza, M., Shibayama, M., Serrano-Luna, J., 2015. *Acanthamoeba castellanii* proteases are capable of degrading iron-binding proteins as a possible mechanism of pathogenicity. *J. Eukaryot. Microbiol.* 62 (5), 614–622.
- Schunder, E., Gillmaier, N., Kutzner, E., Herrmann, V., Lautner, M., Heuner, K., Eisenreich, W., 2014. Amino acid uptake and metabolism of *Legionella pneumophila* hosted by *Acanthamoeba castellanii*. *J. Biol. Chem.* 289 (30), 21040–21054.
- Serrano-Luna Jde, J., Cervantes-Sandoval, I., Calderón, J., Navarro-García, F., Tsutsumi, V., Shibayama, M., 2006. Protease activities of *Acanthamoeba polyphaga* and *Acanthamoeba castellanii*. *Can. J. Microbiol.* 52 (1), 16–23.
- Sidney, L., McIntosh, O., Hopkinson, A., 2015. Phenotypic change and induction of cytokeratin expression during in vitro culture of corneal stromal cells. *Invest. Ophthalmol. Vis. Sci.* 56, 7225–7235.
- Singh, B., Fleury, C., Jalalvand, F., Riesbeck, K., 2012. Human pathogens utilize host extracellular matrix proteins laminin and collagen for adhesion and invasion of the host. *FEMS Microbiol. Rev.* 36, 1122–1180.
- Sissons, J., Alsam, S., Goldsworthy, G., Lightfoot, M., Jarroll, E.L., Khan, N.A., 2006. Identification and properties of proteases from an *Acanthamoeba* isolate capable of producing granulomatous encephalitis. *BMC Microbiol* 6, 42.
- Soto-Arredondo, K.J., Flores-Villavicencio, L.L., Serrano-Luna, J.J., Shibayama, M., Sabanero-López, M., 2014. Biochemical and cellular mechanisms regulating *Acanthamoeba castellanii* adherence to host cells. *Parasitology* 141 (4), 531–541.
- Thornberry, N.A., Lazebnik, Y., 1998. Caspases: enemies within. *Science* 281, 1312–1316.
- Vichai, V., Kirtikara, K., 2006. Sulforhodamine B colorimetric assay for cytotoxicity screening. *Nat. Protoc.* 1, 1112–1116.
- Wang, Z., Wu, D., Tachibana, H., Feng, M., Cheng, X.J., 2020. Identification and biochemical characterisation of *Acanthamoeba castellanii* cysteine protease 3. *Parasit. Vectors* 13, 592.